Journal Name

ARTICLE

Nano-mechanical single-cell sensing of cell-matrix contacts

Lydia Zajiczek,[a] Michael Shaw,[a,b] Nilofar Faruqui,[a] Angelo Bella,[a] Vijay M. Pawar,[b] Mandayam A. Srinivasan[b,c] and Maxim G. Ryadnov[a]*

Received 00th January 20xx,
Accepted 00th January 20xx

DOI: 10.1039/x0xx00000x

www.rsc.org/

Extracellular protein matrices provide a rigidity interface exhibiting nano-mechanical cues that guide cell growth and proliferation. Cells sense such cues using actin-rich filopodia extensions which encourage favourable cell-matrix contacts to recruit more actin-mediated local forces into forming stable focal adhesions. A challenge remains in identifying and measuring these local cellular forces and in establishing empirical relationships between them, cell adhesion and filopodia formation. Here we investigate such relationships using a micromanipulation system designed to operate at the time scale of focal contact dynamics, with the sample frequency of a force probe being 0.1ms, and to apply and measure forces at nano-to-micro Newton ranges for individual mammalian cells. We explore correlations between cell biomechanics, cell-matrix attachment forces and the spread areas of adhered cells as well as their relative dependence on filopodia formation using synthetic protein matrices with a proven ability to induce enhanced filopodia numbers in adherent cells. This study offers a basis for engineering exploitable cell-matrix contacts *in situ* at the nanoscale and single-cell levels.

Introduction

Cell and tissue development rely on the ability of individual cells to sense and exploit extracellular microenvironments.[1,2] Rigidity sensing has a major role in this regard and is critical for the transduction of physical cues to cells.[3] Existing evidence suggests that more rigid substrates promote stable cell adhesion resulting in appreciable cell spreading and proliferation.[4] Such dependence is attributed to focal adhesions which mature better on rigid substrates, while focal contact areas correlate with local cellular forces.[5] To deploy a local force, cells form actin-rich membrane appendages, also known as filopodia. These act as mechanosensors mediating cell contacts with the extracellular matrix (ECM).[6,7] Conversely, it can be said that actin filaments drive the contraction and expansion of the cell membrane necessary for cell locomotion on the ECM.[8] However, cell protrusions displaying filopodia must overcome the resistance of the plasma membrane, which they achieve by bundling >10 actin filaments in each filopodium.[9] Such actin bundles endow filopodia with substantial increases in stiffness in response to external stress.[10] As a consequence, cell-matrix contacts adopt a broken, ellipsoidal, symmetry that allows more actin and adhesion proteins to be recruited to the protruding ends.[11] Enforced by local actomyosin forces this process maintains a constant stress of 5.5 ± 2 nN/μm^2 on focal contacts,[12] which with lateral dimensions not exceeding <500 nm,[13] would elongate with a spring constant of 2.5 nN/μm. Given that the shear detachment forces of cells adhered to the ECM are on the order of 1 μN,[14] cell migration over single-cell distances (≤100 μm) may be expressed with a spring constant of 10 nN/μm. Because the adhesion of an individual cell can be supported by up to 100 focal points, whose formation cycles occur within seconds,[15, 16] their collective force, and by association of filopodia,[17] results in a typical stiffness of 20-40 nN/μm for an adhered cell.[18] This enables fast responses to the substrate cues that stimulate directional motility, with each focal point elongating in a recruiting manner.[5]

Cell recruitment on substrates is most important within the first hours that determine a cell proliferation pattern.[19] For this reason, filopodia emerge as early as in embryos composed of just eight cells to initiate the formation of the first tissue-like layer.[20] Embryonic clusters without filopodia die due to the lack of surface tension which is necessary for cells to expand and contract. Based on all of the above, the challenge of measuring cell recruitment goes beyond individual focal points that are of less importance to cell survival than combined forces of cell stiffness, spreading and attachment,[21, 22] which are directly linked to filopodia formation.[17]

This brings up three requirements. Firstly, to sense cell-matrix interactions requires an approach able to operate at the time scale of focal contact dynamics, i.e. seconds. Secondly, such an approach must able to detect forces exerted by individual cells in the nano-to-micro Newton range. Thirdly, to establish the dependence of cell recruitment on filopodia requires nanostructured protein matrices with a proven ability to induce enhanced filopodia formation in cells. Regarding the first two points, different approaches have been developed to probe the effect of substrate stiffness on cell migration, single-cell adhesion and detachment forces. These include traction force microscopy,[23] cytodetachment,[14] micropipette aspiration,[24] atomic force microscopy (AFM),[25] biomembrane force probe[26] and optical tweezers.[27] Most of these methods however are limited in the

[a]*National Physical Laboratory, Hampton Rd, Teddington, Middlesex, TW11 0LW, (UK) * E-mail: max.ryadnov@npl.co.uk*
[b]*UCL TouchLab, Department of Computer Science, University College London, London, WC1E 6BT (UK)*
[c]*Department of Mechanical Engineering, Massachusetts Institute of Technology, Cambridge MA 02139-4307 (USA)*
† Footnotes relating to the title and/or authors should appear here.
Electronic Supplementary Information (ESI) available: [details of any supplementary information available should be included here]. See DOI: 10.1039/x0xx00000x

range and type of forces that can be measured. Some can only capture focal adhesion dynamics in the early stages of attachment or in highly localized areas of the cell.[28] Force-calibrated microneedles or micropipettes have been used to study the mechanical properties of a wide range of biological structures.[29-31] In contrast to other methods, the advantages of using micropipettes include the application of a greater range of forces appropriate for single-cell-matrix contacts and the ability to measure dynamic interactions.[32] To overcome the limitations of piezo and image-based force sensing methods, such as hysteresis and temperature sensitivity and limited temporal resolution and the need for additional imaging channels, we chose a capacitive based force sensor.[33] In doing so, we were able to match the sensing performance to the range and types of forces needed to measure cell mechanics and substrate binding forces.

More specifically, we developed a novel micromanipulation system comprising a highly sensitive capacitive force transducer mounted on precision piezoelectric stages (Fig 1). The system is capable of directly measuring uniaxial or shear forces involved in single-cell detachment events after several hours of incubation on coated slides over a range of 0.05 – 100 µN. Computer-controlled cell indentation provides repeatable measurements of cell stiffness and detachment forces in the time scale of seconds. Direct and continuous measurements of these characteristics allow for comparison of cell responses to different substrates in biologically relevant conditions.

Regarding the third point, native ECM scaffolds do not normally regulate the extent of filopodia formation. Therefore, we focused on our recently introduced synthetic ECM analogue that takes advantage of mechanistic protein assembly to yield a fibrous, net-like matrix. The matrix, dubbed a self-assembling net (SaNet), uniquely causes increased filopodia numbers in cells when compared to native collagen matrices and ECM adhesion proteins.[34] Another advantage of this synthetic substrate is that it maintains enhanced filopodia formation from the first, early hours of cell adhesion for over a week.[34] To benchmark this effect a native collagen substrate supporting the formation of low filopodia numbers was used as a control. The experiments were performed on both substrates using the primary cell culture of human fibroblasts. These cells are the main structural constituents of connective tissue serving as a stromal framework for functional cells (parenchyma). Therefore, matrix contacts are particularly critical for fibroblasts whose elongation is controlled by mechanosensing at the nanoscale.[15]

Experimental design

Micromanipulation system design

Our micromanipulation system (Fig. 1a) for characterizing the cell-matrix interactions is based around an inverted light microscope (IX-71, Olympus). Glass microscope slides coated with adhered fibroblasts were mounted on a set of manual linear stages with two-dimensional travel over a range of tens of millimetres, allowing for manual location of cells within the field of view of the microscope. A uniaxial force transducer (Aurora 406A, Aurora Scientific Inc.) mounted on a set of high-precision piezoelectric linear stages (ECS industrial line, Attocube) measures the shear force applied to cells during mechanical indentation by a stretched glass capillary tube. An instrument control program written in LabVIEW (National Instruments) allows for the movement of the probe in repeatable, automated sequences of indentations while simultaneously logging the force measured by the probe, the displacement of the probe and capturing phase contrast images of the cell under test. The force transducer uses two variable displacement capacitors to measure compressive and tensile forces from 0 to 500 µN with a nominal sensitivity of 10 nN. An external closed quartz tube is coupled to one of the capacitors, and different tips can be easily attached to and detached from the tube, allowing for flexibility in the size and shape of the probe used.

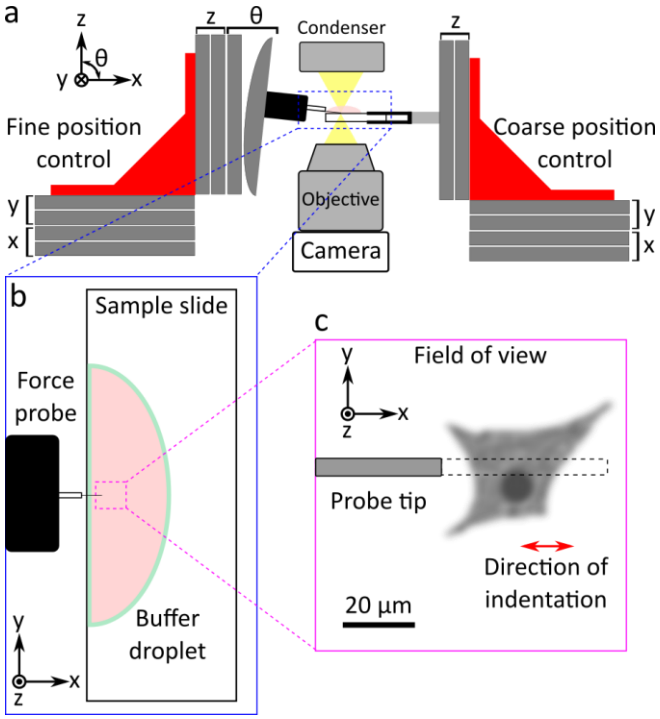

Figure 1. Micromanipulation system design. (a) Schematic diagram showing the micromanipulation system. (b) Magnified view of sample slide showing droplet of a buffer solution formed inside a hydrophobic barrier. (c) The microscope field of view showing a typical indentation sequence.

When operating the transducer in a liquid environment, we find a noise limited sensitivity of approximately 50 nN with a range of 100 µN. The force probe output was calibrated by placing a known reference mass[35] on the quartz tube (without a tip attached) and adjusting the voltage gain and offset of the transducer until the measured force corresponded to the correct value. The piezoelectric stage configuration allows for the three-dimensional positioning of the probe tip with a nominal repeatability of 50 nm, a positioning resolution of encoders being 1 nm and travel of up to 30 mm in each direction through the use of a closed loop positioning controller (ECC100, Attocube). Borosilicate glass capillary tubes (100 µm outside diameter, stretched to 1 – 10 µm diameter points, Capillary Tube Supplies Ltd.) were used as disposable tips and bonded to the quartz tube using a low melting point adhesive (Crystalbond, Agar Scientific). Prior to each experiment, the tip was dipped into a silane solution (99% triisopropylsilane) to further minimize adherence of biological material. The axial stiffness of the capillary tubes is sufficiently high to prevent apparent deformations under the

relatively small forces the tubes are subject to during cell indentation.

Axial stresses transmitted along the capillary tube result in displacement of a fused silica cantilever which forms one of the plates of a variable displacement capacitor. The corresponding force signal is then proportional to an output signal current generated by the transducer drive electronics, which is itself proportional to the difference in capacitance of the force capacitor and an electrically matched reference capacitor mounted beside it. This differential arrangement significantly improves the signal-to-noise ratio by rejection of common mode signals due to thermal effects and mechanical vibration.

Microscope images were acquired with an EMCCD camera (iXon Ultra 897, Andor). Spread cells were imaged with a phase contrast objective (LCACHN 40XPH, Olympus) giving a field of view of 205 µm. Images were captured with a typical frame rate of 10 fps. The three-dimensional probe position and the force transducer output were logged simultaneously; y and z positions were recorded at the image acquisition rate, while x position and force were logged at a higher sampling rate of 10 kHz.

Cell-matrix model and filopodia formation

SaNet is a micrometre-spanning nanofibre net structurally mimicking the native ECM (Fig 2a).[34] The matrix shares the morphological and dimensional characteristics of the ECM including nanoscale structure, network-like assembly and high persistence length.[34] Unlike the ECM or collagen substrates, SaNet does not incorporate known cell recognition motifs (e.g. RGD, YIGSR, IKVAV). Therefore, in the absence of established ligands it is the architecture of the matrix that supports cell proliferation, likely owing to unique filopodia-recognized adhesion points.[6,34]

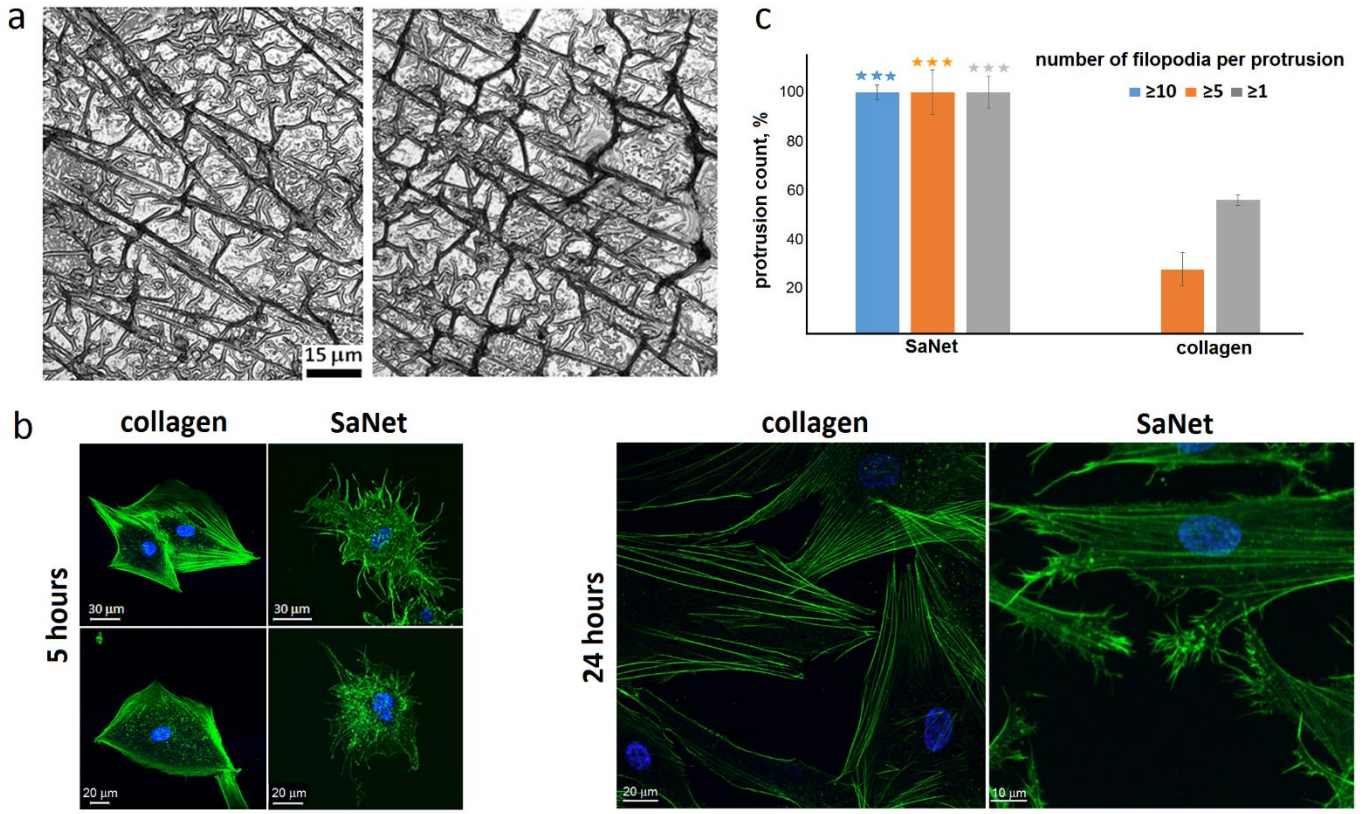

Figure 2. Cell-matrix filopodia-enhancing model using human dermal fibroblasts. (a) Optical micrographs of protein self-assembling nets (SaNet) taken from different areas. (b) Fluorescence micrographs of human dermal fibroblasts stained for F-actin (green) and DNA (blue) grown for 5 hours and 24 hours on collagen and SaNet. (c) Total counts of elongated protrusions with filopodia for 24-hour incubations. The numbers are given in percentage for each substrate are the actual number of filopodia-displaying protrusions divided by the total number of protrusions after subtracting the background number (bare surface). Cells grown on SaNet had significantly ($p < 0.001$) higher numbers of filopodia in comparison to collagen (ANOVA followed by a Fisher post-test for three independent experiments each done in triplicate for each test). Other post-tests used (Tukey, Scheffe and Bonferroni) returned similar p-values.

The adhesion and proliferation of human dermal fibroblasts on this substrate, which were visually monitored by fluorescence microscopy and quantified using cell proliferation assays, gave patterns similar to those of native fibrous collagen and ECM proteins (fibronectin).[34] Compared to collagen, cells on SaNet exhibited greater numbers of filopodia per cell and per elongated protrusion (Fig 2b), while brushed filopodia protrusions (>10 filopodia) were evident only for SaNet (Fig 2c).[34] The effect was already apparent in the first five hours of cell adhesion (Fig 2b,c). In contrast, only moderate filopodia formation was observed for collagen substrates (Fig 2b, c). Thus SaNet and collagen are well suited for a comparative study of cell-matrix contacts as a cumulative function of cell stiffness, attachment and spreading, all of which are physically correlated with actin-rich filopodia.[8-10] More specifically, given the observed differences in filopodia formation, we envisaged that these properties would be enhanced[17] for cells adhered to SaNet when

compared to collagen. To assess this, we monitored the detachment of individual live cells from collagen and SaNet substrates in real time.

Results and discussion

Micromanipulation of live cells on extracellular matrices

To accurately measure cell-interaction forces in nano- to micro-Newton ranges in a liquid environment the probe was moved at a constant average velocity of 70 ± 7 µm/s. This velocity was found to balance the transient effects of viscous drag generated at higher velocities with the stepped nature of the piezo stage at lower velocities. Although nominally uniaxial, the force transducer exhibited a non-zero sensitivity to forces applied perpendicular to the probe (x) axis. Consequently, the submerged tip volume resulted in a buoyancy force offset, which depended roughly linearly on the position of the probe in the droplet. Correction for these underlying variations in measured force was achieved by recording a "reference" indentation at a location close to the cell of interest and subtracting it from the force measured during indentation of the cell itself (Fig S1 and Supporting Information). Over the course of a single experiment, indentation data was collected for individual cells at the various stages of spreading and adhesion. Figure3a shows a typical force trace for the indentation of a cell on SaNet, along with a reference trace, where a negative value indicates compression of the probe (Fig S2). Fig 3b shows the corresponding corrected force-displacement curve and comprises four distinct regions, with corresponding phase contrast images from each region (Fig 3c). In region 1, the force remains constant before contact with the cell is made. Further displacement of the probe results in deformation of the cell (region 2) and an increase in compressive force. The force-displacement curve in this region appears to be linear, suggesting that the material can be characterized by a spring constant.[36] Compressive force decreases in region 3 as focal adhesions are deformed and the cell is gradually detached from the substrate. Finally, in region 4 the cell is fully detached. In this region, the force signal returns to a constant near-zero value (Fig 3b,c), as the detached cell that is adhered to the probe exerts a small buoyant force resulting in a small nonzero shift in the force signal (Video S1).

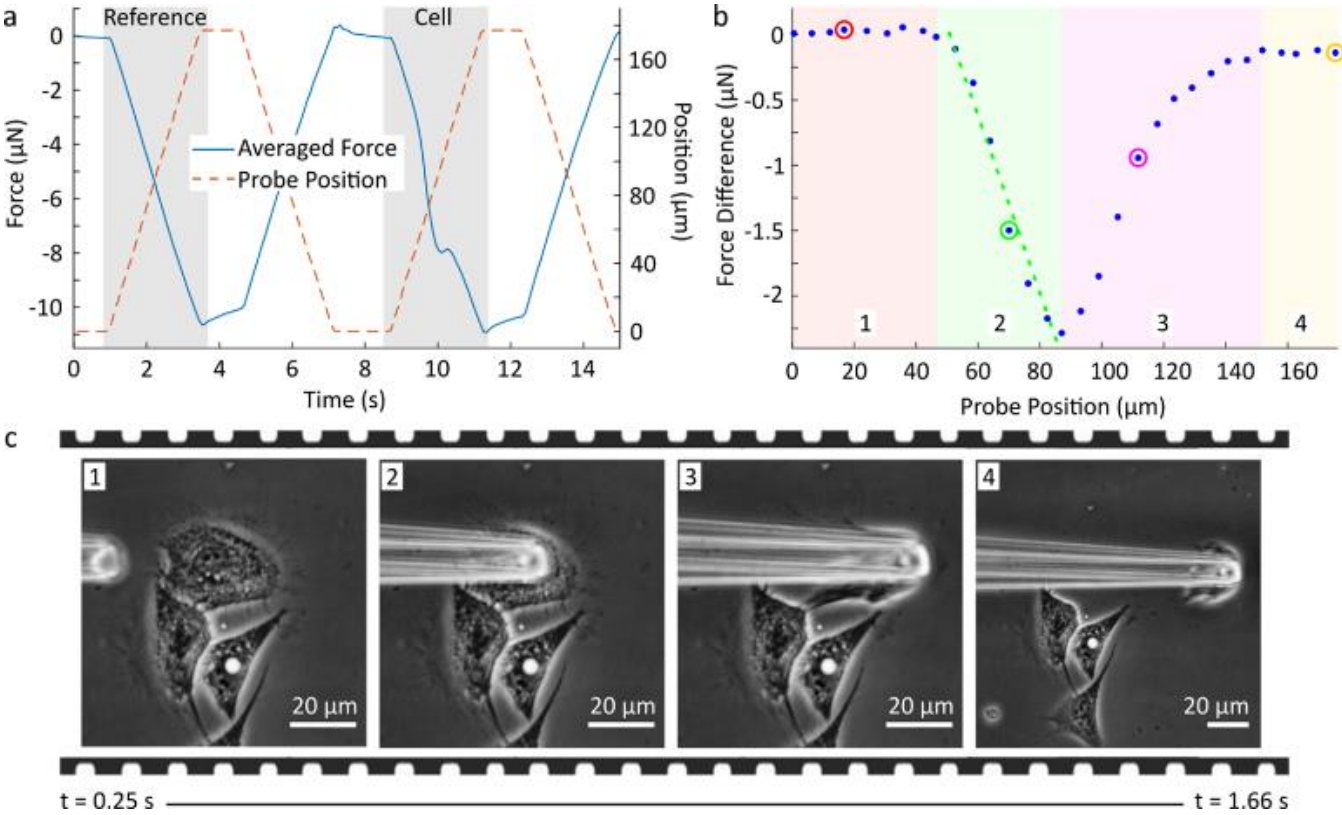

Figure 3. Quantitative measurement of fibroblast biomechanics on SaNet. (a) Measured force (solid blue line) and probe position (dashed orange line) for typical reference and cell indentations. For the reference indentation measured force decreases approximately linearly with time (displacement). (b) Corrected force-displacement signal computed from the difference between force signals recorded during reference and cell indentations. The dotted green line shows fibroblast stiffness extracted in linear compression region. (c) Phase contrast optical micrographs showing an individual cell at different stages of cell indentation. Images correspond to the highlighted points in the force difference plot shown in (b). See also accompanying Video S1.

Comparative quantification of cell-matrix mechanics

Recorded force-displacement curves were analysed[37,38] to determine two main parameters: (1) the cell stiffness defined as the gradient of the force-displacement curve in the linear compression region (region 2) and (2) the detachment force defined as the maximum variation in force over region 2 (Fig 3c). (1) provides a combined measure of cell stiffness and the strength of focal adhesions and (2) is an estimate of the initial detachment force required to break cell-matrix contacts. Both parameters proved to have appreciably larger values for individual cells on SaNet compared to collagen: (1) 59.27 ± 13.64 nN/µm versus 36.18 ± 7.45 nN/µm and (2) 1.51 ± 0.16 µN

versus 0.86 ± 0.18 µN, for SaNet and collagen, respectively. The values for cells on collagen were similar to those typically observed for cells on rigid substrates as well as the native ECM and ECM proteins.[14,18] In this light, the higher values obtained for SaNet, which promotes enhanced filopodia formation, are notable. Filopodia encourage cell spreading and focal adhesions, which increase traction forces,[38] but also stimulate cell motility and more profound attachment-detachment dynamics leading to a higher variance in the measured parameters.[6,17] Indeed, stiffer and more tightly adhered cells on SaNet had a relatively larger footprint area of 3700 µm^2 versus 2900 µm^2 for collagen, while the variance in cell area was higher for cells on SaNet (Fig 4). These findings suggest inter-relationships between cell area and detachment forces or cell stiffness. To determine the significance of these relationships, the Spearman rank correlation was calculated to compare the distribution of values extracted for the two substrates. Detachment forces and cell area were positively correlated for both SaNet (ρ = 0.55) and collagen (ρ = 0.26), while positive correlations between cell stiffness and cell area appeared to be less significant (ρ = 0.27 and ρ = 0.08, respectively).

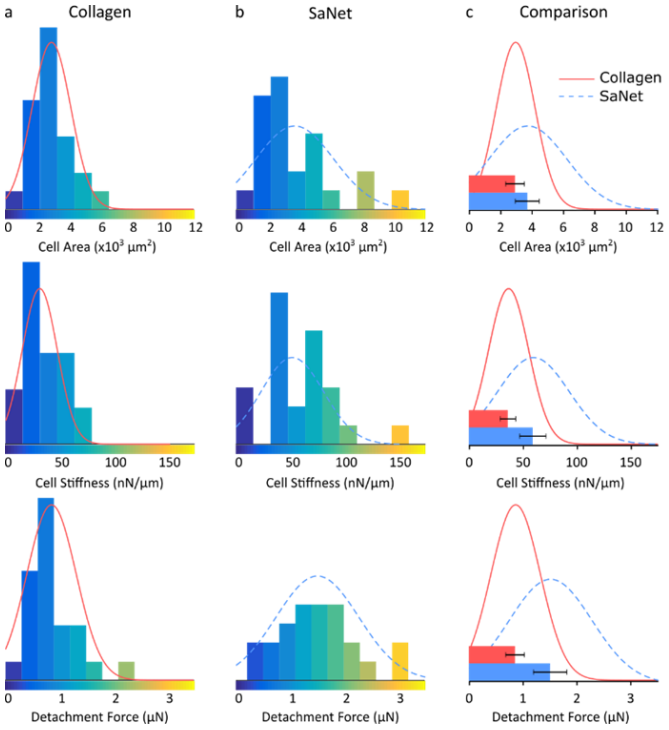

Figure 4. Comparison of measured cell parameters for fibroblasts on different substrates. (a, b) Distribution of measured cell area, detachment force and cell stiffness for human dermal fibroblasts adhered to collagen and SaNet measured for over 25 single cells. Histograms were normalized to show relative frequency, data was binned into 10 intervals and bin widths were equalized. Fitted normal distributions are overlaid. (c) Comparison of distributions for collagen (red solid line) and SaNet (dashed blue line) with bar plots showing mean and standard error of the mean (SEM) for each distribution of values. Cell areas on either substrate were not significantly different ($p < 0.05$). Cells were significantly stiffer ($p < 0.01$) and with a significantly higher detachment force ($p < 0.001$) on SaNet than cells adhered to collagen (ANOVA followed by a Fisher post-test). Other post-tests used (Tukey, Scheffe and Bonferroni) returned similar p-values.

A spreading cell securing a greater number of focal adhesion sites can be expected to exhibit a positive correlation between cell area and detachment force.[38-40] Although precise relationships between cell area, focal adhesions and tensile forces have yet to be established, there appears to be a threshold area above which focal adhesion assembly saturates.[39,41] This is in good agreement with the fact that the collective force of 100 focal points at any given time (down to seconds) supports the adhesion of a single cell,[15-17] which makes the impact of individual adhesion sites that become ruptured during migration and prior to indentation negligible.[42] In contrast, correlations between cell area and cell stiffness are less likely as cell matter density remains constant under elongation.[43] However, since the exact location of indentation on the cell varied between the experiments, variances found in cell stiffness are expected and can be partially attributed to local variations in cytoskeleton stiffness that invariably relate to the varied extent of filopodia formation.[17,44] Consistent with this, the variance in cell stiffness was greater for cells on SaNet, and were correlated with those for detachment forces and cell areas (Fig 4).

The observed differences in the measured forces prompt a conclusion that SaNet supports stronger adhesion due to its profound ability to promote filopodia formation reflecting in greater cumulative cell stiffness and detachment forces (Fig 4). An alternative or complementary contribution of SaNet as a stiffer substrate than collagen is not deemed to have a differential effect. Like collagen and stromal ECMs, SaNet is made of the same constituent material of protein nanofibres that have similar stiffness parameters.[45] In addition, integrin links between extracellular matrices and cellular cytoskeleton, of which there can be 10^4 per cell,[46] operate at lower force ranges (picoN-nN), and alone cannot force-differentiate between different substrates.[47] With no statistically significant differences found in cell area distributions, the significant differences observed in cell stiffness and detachment forces therefore suggest substrate-specific adhesion mechanisms mediated by filopodia recruitment.

Comparative mechanics of stress-accommodating cells

To gain a further insight into to the role of these differences, it was appropriate to probe a specialised cell type with (i) intrinsically broader elasticity values than those of fibroblasts,[48] and (ii) an equally critical dependence on matrix contacts. Bone-generating human osteoblasts appeared as an excellent model, for which similar force-displacement curves were recorded (Fig S3a,b & Video S2).

Regarding (i), osteoblasts exhibit significant variability in elasticity (0.3-20 kPa),[49] which helps them to accommodate to a broad range of externally applied stress without changing cell morphology or area.[50] This property is likely to allow osteoblasts to adopt similar footprints on both studied matrices. In line with this, osteoblasts on SaNet and collagen had nearly identical footprint areas, 2100 µm^2 and 2300 µm^2, respectively, while showing similar variances with no significant differences in statistical distributions (ρ = 0.53). The smaller cell areas for osteoblasts were consistent with osteoblasts being stiffer and more compact than fibroblasts.[49,50] This finding is therefore notable for two reasons. Firstly, it strongly suggests that a relative ratio in cell stiffness values for osteoblasts on the two matrices should be reduced when compared to that for fibroblasts. This was indeed observed. The values for fibroblasts (59 nN/µm

versus 36 nN/µm) related at 1.6 ratio, whereas a much closer ratio of 1.2 was derived from cell stiffness values, albeit expectedly higher (70 nN/µm versus 57 nN/µm on SaNet and collagen, respectively), for osteoblasts. Secondly, with the cell area being essentially constant, this ratio should be and was supported by comparable correlations between detachment force and cell stiffness, which for SaNet and collagen were ρ = 0.87 and ρ = 0.82, respectively.

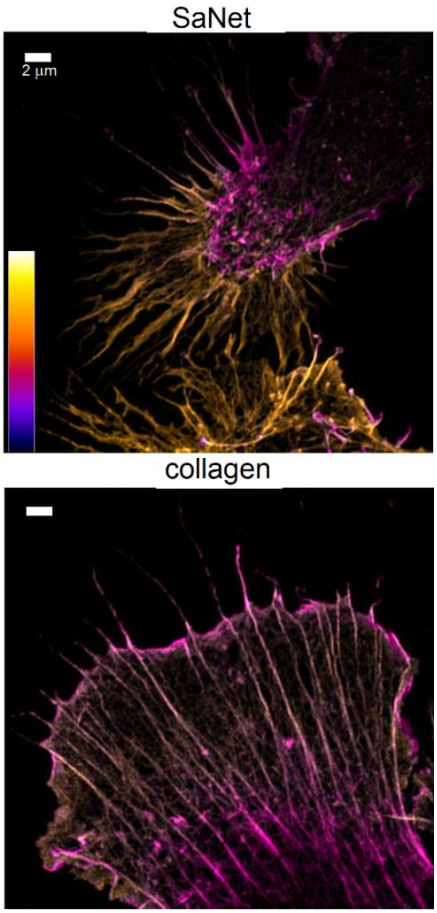

Figure 5. Filopodia formation on osteoblasts. Fluorescence super-resolution micrographs of osteoblasts that were actin-stained with phalloidin-Alexa Fluor 488 following incubation on SaNet and collagen (24 hours). The images are colour coded depth projections to distinguish between cytoskeleton actin in lamellipodia projections (violet) and filopodia extending from lamellipodia (orange). Depth colour scale is 1 µm.

Based on the above and regarding (ii), this ratio can be used as a quantitative measure to express the strength with which an experimental matrix may promote cell adhesion. In this case, collagen serves as a reference matrix to benchmark the experimental matrix, while ratio values above and below 1 respectively indicate enhanced and impaired adhesion properties of the assessed matrix.

A question however remains as to what encourages stiffer osteoblasts on SaNet. In fibroblasts increased stiffness was linked to enhanced filopodia formation, while in osteoblasts the same effect has not been shown before. Intriguingly, the very force measurements performed on osteoblasts revealed evident filopodia formation (Fig S3b, c & Video S2). A more detailed super-resolution[51] analysis of the same samples confirmed remarkably abundant filopodia projections for osteoblasts on SaNet, which was in marked contrast to cells cultured on collagen (Fig 5). These results strengthen the earlier conclusion of that SaNet promoted stronger adhesion by inducing enhanced filopodia formation. The phenomenon thus appears to be a likely deferential factor for force dynamics on different matrices. To further support this conjecture, the measured cell parameters obtained on the reference matrix collagen were compared for the two cell types (Fig S4). The variance analysis confirmed that cell areas were not significantly different between the two types, while osteoblasts remained significantly stiffer than fibroblasts. Collectively, these findings indicate that SaNet induces profound filopodia formation leading to increases in cell stiffness without necessarily having impact on the footprint areas of cells with intrinsically broader variations in elastic modulus.

Because filopodia are actin-rich cellular projections, all the observed differences and deduced correlations are pre-determined by normal actin polymerisation at early stages.[52] At least partly, this proved to be the case in our studies. Specifically, cells treated with an actin-depolymerising drug latrunculin underwent immediate detachment from collagen requiring forces at a lowest observed range of 0.63 ± 0.12 µN. The effect was in good agreement with the reduced areas of such cells which did not exceed 500-1000 µm^2, suggesting significantly compromised adhesion abilities.

Conclusions

Despite their importance for cell growth and development, the dynamics of cell-matrix adhesions remain challenging to capture, let alone to understand fully. Partly, the problem is technical as it requires an approach capable of routine force measurements at the time and length scales of single-cell focal adhesions. Not only should such measurements be able to register force differences at the nano-to-micro Newton ranges, but they should do so for individual live, as opposed to fixed, cells in native and near-native environments.

In this regard, our micromanipulation system provides a capability that measures biomechanical properties of live cells during cell indentations with time in biologically relevant conditions over a much larger range of forces and their distribution than the current state of the art methods allow.[23-33] The system can visually assess the deformations of the contact area to understand the force distribution upon, during and after contact.

For another part, the problem comes down to finding suitable extracellular matrix models that given the nature and purpose of the measurements would help emphasise the physical rather than biochemical rationale of cell recruitment. Using a synthetic, non-biological, collagen-like mimetic we have shown that physical forces regulating cell-matrix contacts can be measured differentially and correlatively during the time of cell displacement and at the nanoscale. Exemplified by a natural biophysical phenomenon, filopodia formation, our approach provided evidence for more appreciable cell recruitment as a function of stronger cell-matrix contacts supported by enhanced filopodia formation. By extracting empirical correlations between cell stiffness, detachment force and cell area we established that cells directly respond to morphological and physical variations in extracellular matrices. These responses are reflected in increased forces cells apply to the sensed matrix points suggesting enhanced actin-rich recruitment in focal adhesions.

All in all, our findings offer a basis for engineering exploitable cell-matrix contacts *in situ* at the single-cell and nanoscale levels. The results are anticipated to underpin searches for more subtle correlations, at the molecular and near-atomistic levels, which may reveal molecular or morphological patterns on nanofibre matrix surfaces as potential non-biological determinants for differential cellular responses.[34,53]

Acknowledgements

We thank Muna Elmi for the preparation of probe tips and Stuart Davidson for assistance in calibration of the force transducer. This work was funded by the European Research Council (grant ERC-AdG-247401), the UK's Engineering and Physical Sciences Research Council (grant EP/K005030/1) and the strategic research programme of the UK National Measurement System.

Notes and references

1. B. M. Gumbiner, Cell, 1996, 84, 345–357.
2. E. D. Hay, Cell Biology of Extracellular Matrix, Springer Science & Business Media, New York, 2nd edn., 1991, vol. 2.
3. D. E. Discher, P. Janmey and Y.-L. Wang, Science, 2005, 310, 1139–43.
4. K. Bhadriraju and L. K. Hansen, Exp. Cell Res., 2002, 278, 92–100.
5. C.-M. Lo, H.-B. Wang, M. Dembo and Y. Wang, Biophys. J., 2000, 79, 144–152.
6. C. A. Heckman and H. K. Plummer, Cell. Signal., 2013, 25, 2298–2311.
7. P. W. Oakes and M. L. Gardel, Curr. Opin. Cell Biol., 2014, 30, 68–73.
8. J. C. M. Mombach and J. A. Glazier, Phys. Rev. Lett., 1996, 76, 3032–3035.
9. M. J. Footer, J. W. J. Kerssemakers, J. A. Theriot and M. Dogterom, Proc. Natl. Acad. Sci., 2007, 104, 2181–2186.
10. M. L. Gardel, J. H. Shin, F. C. MacKintosh, L. Mahadevan, P. Matsudaira and D. A. Weitz, Science, 2004, 304, 1301–5.
11. D. Riveline, E. Zamir, N. Q. Balaban, U. S. Schwarz, T. Ishizaki, S. Narumiya, Z. Kam, B. Geiger and A. D. Bershadsky, J. Cell Biol., 2001, 153, 1175–1186.
12. N. Q. Balaban, U. S. Schwarz, D. Riveline, P. Goichberg, G. Tzur, I. Sabanay, D. Mahalu, S. Safran, A. Bershadsky, L. Addadi and B. Geiger, Nat. Cell Biol., 2001, 3, 466–472.
13. A. I. Teixeira, G. A. Abrams, P. J. Bertics, C. J. Murphy and P. F. Nealey, J. Cell Sci., 2003, 116, 1881–92.
14. A. Yamamoto, S. Mishima, N. Maruyama and M. Sumita, J. Biomed. Mater. Res., 2000, 50, 114–124.
15. M. Prager-Khoutorsky, A. Lichtenstein, R. Krishnan, K. Rajendran, A. Mayo, Z. Kam, B. Geiger and A. D. Bershadsky, Nat. Cell Biol., 2011, 13, 1457–1465.
16. J. P. Califano and C. A. Reinhart-King, Cell. Mol. Bioeng., 2010, 3, 68–75.
17. S. Wong, W.-H. Guo and Y.-L. Wang, Proc. Natl. Acad. Sci., 2014, 111, 17176–17181.
18. K. Hayashi, in Mechanics of Biological Tissue, eds. G. A. Holzapfel and R. W. Ogden, Springer Science & Business Media, New York, 2006, pp. 135–152.
19. T. Diu, N. Faruqui, T. Sjöström, B. Lamarre, H. F. Jenkinson, B. Su and M. G. Ryadnov, Sci. Rep., 2014, 4, 7122.
20. J. C. Fierro-González, M. D. White, J. C. Silva and N. Plachta, Nat. Cell Biol., 2013, 15, 1424–1433.
21. C. G. Galbraith, K. M. Yamada and M. P. Sheetz, J. Cell Biol., 2002, 159, 695–705.
22. C. Grashoff, B. D. Hoffman, M. D. Brenner, R. Zhou, M. Parsons, M. T. Yang, M. A. McLean, S. G. Sligar, C. S. Chen, T. Ha and M. A. Schwartz, Nature, 2010, 466, 263–266.
23. M. R. Ng, A. Besser, G. Danuser and J. S. Brugge, J. Cell Biol., 2012, 199, 545–63.
24. R. M. Hochmuth, J. Biomech., 2000, 33, 15–22.
25. A. M. Collinsworth, S. Zhang, W. E. Kraus and G. A. Truskey, Am. J. Physiol. Cell Physiol., 2002, 283, C1219–27.
26. E. Evans, K. Ritchie and R. Merkel, Biophys. J., 1995, 68, 2580–2587.
27. O. Thoumine, P. Kocian, A. Kottelat and J. Meister, Eur. Biophys. J., 2000, 29, 398–408.
28. A. Khalili and M. Ahmad, Int. J. Mol. Sci., 2015, 16, 18149–18184.
29. J. Howard and A. J. Hudspeth, Proc. Natl. Acad. Sci. USA, 1987, 84, 3064-3068.
30. M. Okuno and Y. Hiramoto, J. Exp. Biol., 1979, 79, 235-243.
31. G. W. Francis, L. R. Fisher, R. A. Gamble and D. Gingell, J Cell Sci. 1987, 87, 519-523.
32. Y. Shimamoto and T. M. Kapoor, Nat Protoc., 2012, 7, 959-969.
33. Y. Sun and B. J. Nelson, Biomed. Mater., 2007, 2, 16-22.
34. N. Faruqui, A. Bella, J. Ravi, S. Ray, B. Lamarre and M. G. Ryadnov, J. Am. Chem. Soc., 2014, 136, 7889–98.
35. S. Davidson, J. Berry and K. Marti, Vacuum, 2015, 120, 139–146.
36. S. Y. Tee, A. R. Bausch and P. A. Janmey, Curr. Biol., 2009, 19, 745–748.
37. D. J. Hudson, J. Am. Stat. Assoc., 1966, 61, 1097–1129.
38. S. J. Han, K. S. Bielawski, L. H. Ting, M. L. Rodriguez and N. J. Sniadecki, Biophys. J., 2012, 103, 640–648.
39. T. Luo, K. Mohan, P. A. Iglesias and D. N. Robinson, Nat. Mater., 2013, 12, 1064–1071.
40. A. Pietuch and A. Janshoff, Open Biol., 2013, 3, 130084.
41. N. D. Gallant, K. E. Michael and A. J. García, Mol. Biol. Cell, 2005, 16, 4329–40.
42. A. J. Ridley, M. A. Schwartz, K. Burridge, R. A. Firtel, M. H. Ginsberg, G. Borisy, J. T. Parsons and A. R. Horwitz, Science, 2003, 302, 1704–9.
43. J. Brevier, M. Vallade and D. Riveline, Phys. Rev. Lett., 2007, 98, 268101.
44. V. M. Laurent, S. Kasas, A. Yersin, T. E. Schäffer, S. Catsicas, G. Dietler, A. B. Verkhovsky and J.-J. Meister, Biophys. J., 2005, 89, 667–75.
45. M. P. E. Wenger, L. Bozec, M. A. Horton and P. Mesquida, Biophys. J., 2007, 93, 1255–1263.
46. S. Benedetto, R. Pulito, S. G. Crich, G. Tarone, S. Aime, L. Silengo and J. Hamm, Magn. Reson. Med., 2006, 56, 711–716.
47. G. Jiang, G. Giannone, D. R. Critchley, E. Fukumoto and M. P. Sheetz, Nature, 2003, 424, 334–337.
48. T. G. Kuznetsova, M. N. Starodubtseva, N. I. Yegorenkov, S. A. Chizhik, R. I. Zhdanov, Micron, 2007, 38, 824-833.
49. A. Simon, T. Cohen-Bouhacina, M.C. Porté, J. P. Aimé, J. Amédée, R. Bareille, C. Baquey, Cytometry A. 2003, 54, 36-47.
50. M. J. Jaasma, W. M. Jackson and T. M. Keaveny, Ann Biomed

Eng., 2006, 34, 759-768.
51. M. Shaw, L. Zajiczek and K. O'Holleran, Methods, 2015, 88, 11-19.
52. T. Wakatsuki, B. Schwab, N. C. Thompson and E. L. Elson, J Cell Sci. 2001, 114, 1025-36.
53. M. G. Ryadnov and D. N. Woolfson, Nat. Mater., 2003, 2, 329-332.

